ORIGINAL ARTICLE

Host–guest complexes of various cucurbit[n]urils with the hydrochloride salt of 2,4-diaminoazobenzene

Zhi-Fang Fan · Juan Wang · Ying Huang ·
Sai-Feng Xue · Xin Xiao · Yun-Qian Zhang ·
Qian-Jiang Zhu · Zhu Tao

Abstract The interaction products of normal cucurbit[n]urils (n = 7, 8; Q[7] Q[8]) and a sym- tetramethyl-substituted cucurbit[6]uril derivative (TMeQ[6]) with the hydrochloride salts of 2,4-diaminoazobenzene (**g**·HCl) were investigated in aqueous solution using ^{1}H NMR spectroscopy, electronic absorption spectroscopy, as well as single crystal X-ray diffraction. The ^{1}H NMR spectra analysis established a basic interaction model in which inclusion complexes with a host:guest ratio of 1:1 form for the TMeQ[6] and Q[7] cases, while they form with a host:guest ratio of 1:2 for the Q[8] case. Commonly, the hosts selectively bound to the phenyl moieties of the guests. Absorption spectrophotometric analysis in aqueous solution defined the stability of the host–guest inclusion complexes at pH 3.2. Quantitatively, at this pH, complexes with a host:guest ratio of 1:1—those with smaller hosts TMeQ[6] and Q[7]—formed with logK values between 6 and 7. That with host Q[8] and a host:guest ratio of 1:2 formed with a logK value of 10.8. Single crystal X-ray structures of the inclusion complexes TMeQ[6]–**g**·HCl and Q[8]–**g**·HCl showed the phenyl moiety of the guest inserted into the host cavity. This result supports the solution-based ^{1}H NMR spectroscopic study.

Z.-F. Fan · J. Wang · Y. Huang · S.-F. Xue (✉) · X. Xiao ·
Y.-Q. Zhang · Q.-J. Zhu · Z. Tao
Key Laboratory of Macrocyclic and Supramolecular Chemistry
of Guizhou Province, Guizhou University, Guiyang 550025,
People's Republic of China
e-mail: sfxue@gzu.edu.cn
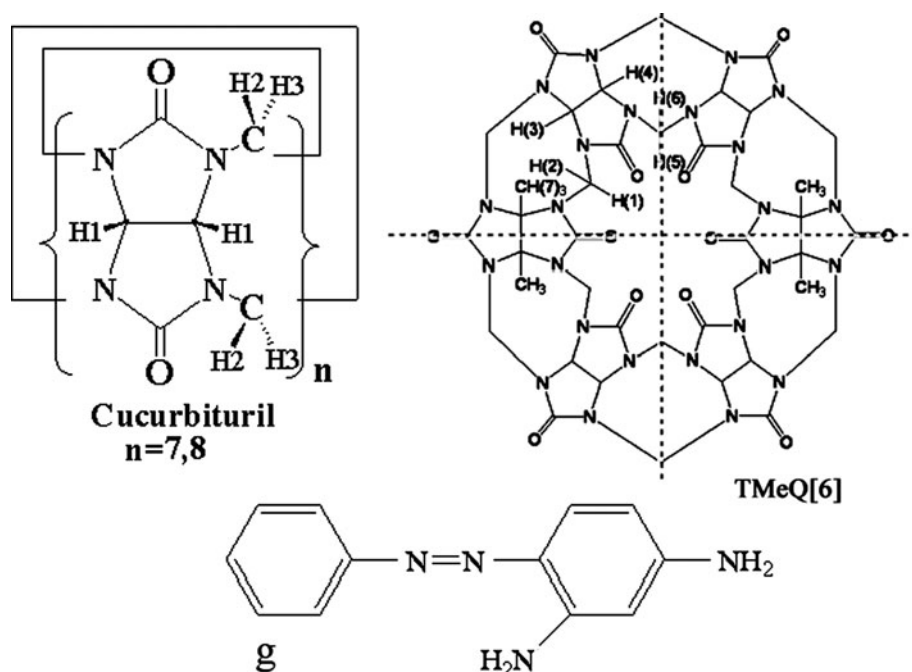
Introduction

The cucurbit[n]uril (Q[n]) compounds are a relatively new receptor family with common characteristic features including a hydrophobic cavity and polar carbonyl groups surrounding the opening portals. Among other examples, the structure of cucurbit[6]uril (Q[6]) was first determined and reported by Mock and coworkers [1]. About two decades later, in 2000 homologues cucurbit[n = 5, 7, 8]urils (Q[5], Q[7], Q[8]) were synthesized and reported almost at the same time by two groups [2, 3]. Synthesis of cucurbit[10]uril (Q[10]), formed along with Q[5], was reported in 2002 [4]. In 2004, a symmetrical substituted cucurbit[n]uril, α, α', δ, δ' tetramethylcucurbit[6]uril (TMeQ[6]) [5], which possessed excellent water solubility, was first synthesized in our laboratory by using the dimmer of glycoluril, which was characterized later by our group and the Isaacs's group at almost the same time [6, 7] and the diether of dimethyl-glycoluril. We also investigated the host–guest chemistry of TMeQ[6] in neutral water [5] (Fig. 1). The varying cavity and portal sizes available in Q[n] molecules, and particularly their ability to form inclusion or exclusion complexes with organic species or inorganic ions, have led to considerable research focus on uncovering the remarkable molecular recognition properties which can provide a building block for supramolecular chemistry. Some of this work has been summarized in recent reviews [8–14].

Dye contamination of water bodies in developing nations is a serious problem. Dyes are released to the environment from two major sources, namely the textile and dyestuff

Fig. 1 Structures of the host and the guest used in this work

industries. In order to be useful, typical synthetic dyes must be highly stable to light and washing, and resistant to microbial attack [15]. These dyes do not, therefore, readily degrade and are not removed from the effluent by conventional wastewater treatment methods [16]. Azo dyes are the largest class of dyes, with the greatest variety of colors [17]. They also exhibit great structural variety and therefore, as a group, they are not uniformly susceptible to microbial attack [15]. Azo dyes, most predominantly sulfonated azo dyes, constitute 84% of all dyes used.

2,4-diaminoazobenzenes, which are potentially carcinogenic, have been widely used in the manufacture of dyes and pigments for cloth, paper, and leather, 2,4-diaminoazobenzenes are discharged by the dye industry and are often released in effluent waste water, leading to their presence in lakes, rivers and soils [18]. In the 1990s, Buschmann and coworkers investigated the decolorization, or selective removal, of different dyes from solutions, using water-insoluble Q[6] precipitated on a carrier material or dissolved in formic acid. Nevertheless, few structural details of the Q[n]-dyes were reported [19].

In this work, we compared a water-soluble sym-tetramethyl-substituted cucurbit[6]uril (TMeQ[6]), with normal Q[7] and Q[8]. We investigated the details of their interaction with the hydrochloride salt of 2,4-diaminoazobenzene (g·HCl), by using X-ray crystal structure analysis, ^{1}H NMR spectroscopy and electronic absorption spectroscopy (Fig. 1). The guest was composed of two aromatic moietiesphenyl and benzenediamine rings-both of which were small enough to allow inclusion in the cavity of the selected hosts or of its substituted derivatives [20–24]. Our

work demonstrated not only a 1:1 interaction model, exemplified by the interaction of TMeQ[6] or Q[7] with the guest, but also a 1:2 interaction model, exemplified by the interaction of Q[8] with the guest.

Experimental

Materials

TMeQ[6], Q[7], and Q[8] were prepared and purified according to the method developed in our laboratories [7]. Analytical grade 2,4-diaminoazobenzene hydrochloride (g·HCl) was obtained from Shanghai Chongming Chemical Co., Ltd., and used without further purification.

^{1}H NMR titrations

2.0–2.5 × 10^{-3} mmol samples of Q[n] in 0.5–0.7 g D$_2$O, with guest:Q[n] ratios ranging between 0.5 and 6, were prepared for the study of host–guest complexation between Q[n] and the title guest. The ^{1}H NMR spectra were recorded at 20 °C on a Varian INOVA-400 spectrometer.

Absorption study

Aqueous solutions of HCl salts of the guest were prepared in a concentration of 1 × 10^{-3} mol/L. Aqueous solutions of the hosts were prepared in a concentration of 1 × 10^{-4} mol/L. These stock solutions were combined to

give solutions containing a fixed guest concentration of 2.0×10^{-5} mol/L in each solution with a guest:Q[n] ratio of 0, 0.2:1, 0.4:1, 1:1, 1.5:1, 2:1…, and each solution was characterized by absorption spectroscopy. The pH of the solutions was adjusted using HCl and closed to 3.2 at which both of the free guest and the bound guest were protonated. UV–visible (UV–Vis) absorption spectra of the host–guest complexes were recorded on an Agilent 8453 spectrophotometer at room temperature.

X-ray crystallography

Preparation of (TMeQ[6]–**g**)·Cl·5(H$_2$O) (**1**): A single crystal of the TMeQ[6] adduct with **g** (as shown in Fig. 1) was obtained by dissolving TMeQ[6] (0.20 g, 0.19 mmol) in a solution of **g**·HCl (0.047 g, 0.20 mmol) in water (5 mL). The final solution was mixed thoroughly and allowed to stand at room temperature. Crystals suitable for X-ray diffraction were formed after several days. (FW = 1391.79) Anal. Calcd. for **1**: C,44.88; H, 4.85; N, 28.10. Found: C, 43.93; H, 4.96; N, 27.68.

Preparation of (Q[8]–2**g**)·2Cl·14(H$_2$O) (**2**): A single crystal of the Q[8] adduct with **g** was obtained by dissolving Q[8] (0.29 g, 0.19 mmol) in a solution of **g**·HCl (0.047 g, 0.20 mmol) in water (5 mL). The insoluble residue was filtered, and the filtration was allowed to stand at room temperature. Crystals suitable for X-ray diffraction formed after several days. (FW = 2078.84) Anal. Calcd. for **2**: C,41.60; H, 4.955; N, 26.97. Found: C,40.86; H, 5.05; N; N, 26.53.

Experimental data were collected for compounds **1** and **2** on a Bruker APEX2 CCD diffractometer (graphite monochromatized, MoKα-radiation, ω and φ scan mode, 10 s frame-1). The structures of compounds **1** and **2** were solved and refined using anisotropic thermal parameters for all non-hydrogen atoms. The hydrogen atoms belonging to the host and guest were placed in calculated positions and further refined using the riding model. Hydrogen atoms in the water molecules were not located from the difference electron density map. All the refinements were performed using SHELXTL-Plus software. CCDC reference numbers 718845 for compound 1 and 718846 for compound 2.

Crystal data for compound 1: [(C$_{40}$H$_{44}$N$_{24}$O$_{12}$)(C$_{12}$H$_{13}$N$_2$)]· Cl·5(H$_2$O), $M = 1391.79$, triclinic, $a = 12.0591(8)$ Å, $b = 13.3323(9)$ Å, $c = 24.3017(17)$ Å, $\alpha = 104.456(3)°$, $\beta = 92.714(3)°$, $\gamma = 73.900(8)°$, $V = 3765.7(4)$ Å^3, $T = 223.0(2)$ K, space group P-1 (no.2), $Z = 2$, $\lambda(\mathrm{MoK}\alpha) = 0.71073$ Å, $\mu(\mathrm{MoK}\alpha) = 0.128$ mm^{-1}, 12818 reflections measured, 7204 unique ($R_{\mathrm{int}} = 0.0468$) which were used in all calculations. The final R_1 and wR_2 were 0.0813 and 0.2417 for I > 2σ(I), 0.1245 and 0.2682 for all data.

Crystal data for compound 2: [(C$_{48}$H$_{48}$N$_{32}$O$_{16}$)(C$_{12}$H$_{13}$N$_4$)$_2$]·2Cl·14(H$_2$O), $M = 2078.84$, monoclinic,

$a = 14.471(7)$ Å, $b = 22.919(11)$ Å, $c = 16.135(8)$ Å, $\alpha = 90.00°$, $\beta = 105.023(7)°$, $\gamma = 90.00°$, $V = 5169(4)$ Å^3, $T = 223.0(2)$ K, space group P2$_1$/c (no. 14), $Z = 2$, $\lambda(\mathrm{MoK}\alpha) = 0.71073$ Å, $\mu(\mathrm{MoK}\alpha) = 0.155$ mm^{-1}, 8679 reflections measured, 3750 unique ($R_{\mathrm{int}} = 0.0984$) which were used in all calculations. The final R_1 and wR_2 were 0.0841 and 0.2112 for I > 2σ(I), 0.1740 and 0.2498 for all data.

Results and discussion

^{1}H NMR spectra analysis of the interaction between the Q[n]s with g·HCl

Figure 2 shows the ^{1}H NMR spectra for **g**·HCl recorded in the absence (a) and in the presence of TMeQ[6] with increasing concentration (b–f). Figure 3 shows spectra for **g**·HCl recorded in the absence (a) and in the presence of Q[7] with increasing concentration (b–f). Figure 4 shows spectra for **g**·HCl recorded in the absence (a) and in the presence of Q[8] with increasing concentration (b–d).

One can see two sets of resonance signals of the bound and unbound **g**·HCl, and the strengths of them change with the increase of the concentration of the host TMeQ[6]. Meanwhile, the two sets of the resonance of methyl protons show clearly the bound and unbound TMeQ[6] in the equilibrium of the interaction of the TMeQ[6] and the guest **g**·HCl in Fig. 2. The signals corresponding to the bound **g**·HCl were present after addition of 0.60 equivalent of TMeQ[6] (Fig. 2b). The resonances of the phenyl ring of the guest were shifted upfield by at least δ 0.79 (as indicated by the red arrowhead), while the rest of ring resonances (H^1–H^3) were shifted significantly downfield by δ 0.1–0.8 (as indicated by the red arrowhead). This suggests that the phenyl ring of the guest was in the shielding zone in the cavity of the host, while the m-phenylenediamine ring was in the deshielding zone at the portal of the host. This conclusion was further verified by the crystal structure of the inclusion complex of TMeQ[6]–**g**·HCl (Fig. 6).

Titration spectra show that only one set of resonance signals of the **g**·HCl which underwent a gradually shift upfield (H$^{4-6}$) or downfield (H^3) with increasing equivalents of host Q[7], it suggests that can include g1 into its cavity with a fast ingress and egress exchange ratio (cases b–d in Fig. 3). In particular, at higher host:guest ratios (up to 6.07 in Fig. 3f), resonance signals of protons (H$^{4-6}$) of the guest exhibited a upfield shift by ~0.7–0.8 ppm, while the resonance signal of proton (H^3) of the guest exhibited a upfield shift by ~0.5 ppm respectively. This suggests that the phenyl ring of the guest was included in the cavity of the host, while the m-phenylenediamine ring was excluded in the portal zone of the host. Although chemical shift

Fig. 2 The ^{1}H NMR spectra of **g**·HCl recorded **a** in the absence and **b–e** TMeQ[6]–**g**·HCl system with increasing concentration of TMeQ[6], **f** TMeQ[6]
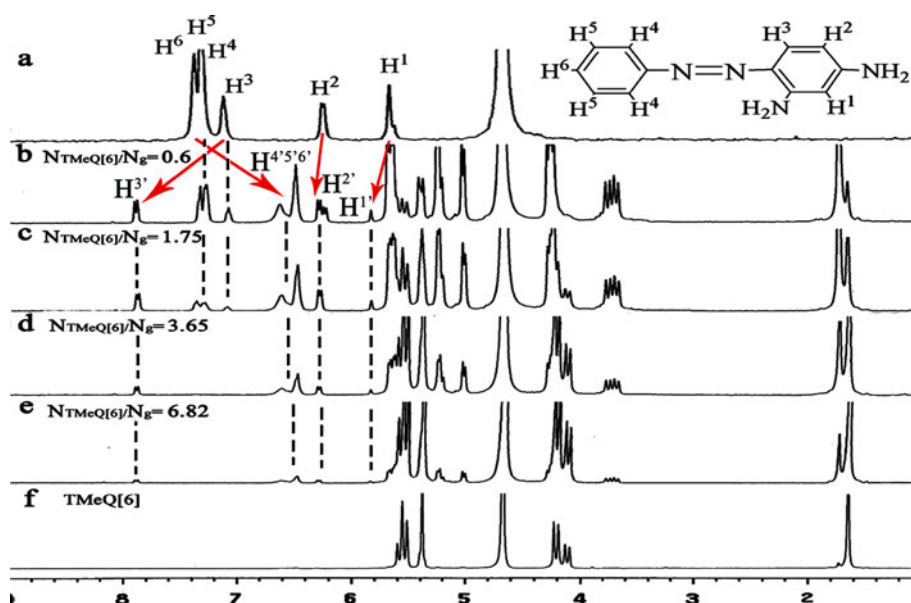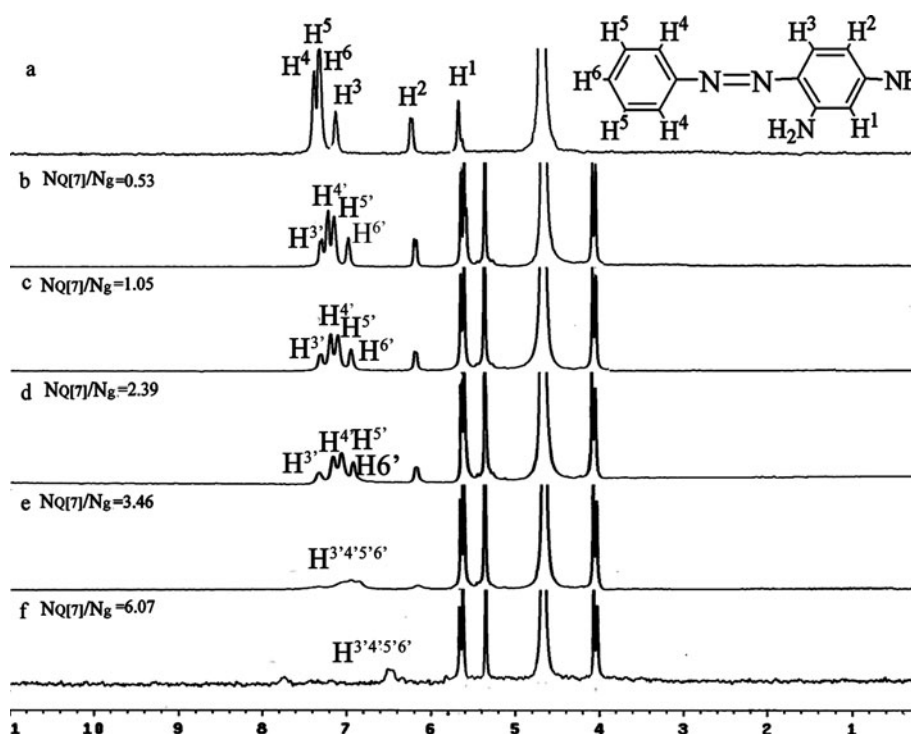

Fig. 3 The ^{1}H NMR spectra of **g**·HCl recorded **a** in the absence and **b–f** Q[7]–**g**·HCl system with increasing concentration of Q[7]

changes of certain proton resonances of the guest or host with increasing or decreasing equiv of the guest or host can be used to study host–guest interaction, it was difficult to read the accurate chemical shift and the integrity of the guest for the Q[7]–**g** interaction system due to the broad proton resonances of the guest.

Unlike TMeQ[6]–**g** or Q[7]–**g** interaction systems, in which the hosts are water soluble and ^{1}H NMR titration experiments are performed by adding a guest solution into a host solution gradually. For the Q[8]–**g** interaction system,

the titration spectra were obtained by adding solid of Q[8] into the guest solution gradually due to the poor solubility of the host Q[8] (Fig. 4b–d). The very broad proton resonances of the guest, in particular at a lower $N_{Q[8]}/N_g$ ration (Fig. 4b), indicate a fast exchange on the NMR time scale so that it was difficult to read the accurate chemical shift and the integrity of the guest for the Q[8]–**g** interaction system. However, the proton resonances of the phenyl ring were clearly shifted upfield (Fig. 4c, d), suggesting the phenyl ring of the guest was in the cavity of the host Q[8].
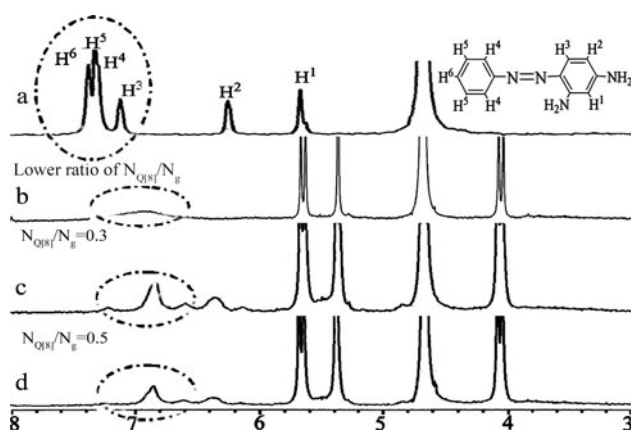
Fig. 4 The ^{1}H NMR spectra of **g**·HCl recorded **a** in the absence and **b–d** Q[8]–**g**·HCl system with increasing concentration of Q[8]

Spectrophotometric analysis of the interaction between Q[n]s and g·HCl

To further quantify the interaction between the various Q[n] and **g**·HCl in solution, a ratio-dependent study was pursued by monitoring electronic absorption. In acid solution, the protonated form of the **g**·HCl prevails, having the characteristic absorption peak at 456 nm. The changes in the absorption spectra of the g·HCl as a function of pH of the solution are shown in the Fig. 1S (see the supporting information). Based on the ground state pKa of the **g**·HCl, we adjusted the pH of related solutions near 3 to study the complexation of the protonated form of the guest with the hosts (Fig. 5).

Usually, the hosts Q[n] showed no absorbance for $\lambda > 210$ nm, and the free HCl salt of the guest showed maximum absorption at $\lambda_{max} = 456$ nm in **g**·HCl. Fig. 5a–f show the variation in the UV spectra obtained from aqueous solutions containing a fixed concentration of **g**·HCl $(2.0 \times 10^{-5}$ mol/L), with variable concentrations of Q[n]s repectively. The addition of TMeQ[6] to a solution of **g**·HCl at pH 3.2 results in decreasing absorption with a bathochromic shift from 456 to 461 nm (Fig. 5a). The relationship between absorbance (A) at $\lambda_{max} = 456$ nm and molar ratio of host TMeQ[6] to guest $(N_{TMeQ[6]}/N_{g·HCl})$ can be fitted to a 1:1 binding model for the TMeQ[6]–**g**·HCl systems (Fig. 5b), and this stoichiometry is also confirmed by a Job's plot (Fig. 5b inset). The Q[7]–**g**·HCl system shows similar variation of absorption bands upon addition of Q[7] to an aqueous solution of **g**·HCl at pH 3.2 with a bathochromic shift from 456 nm to 459 nm (Fig. 5c). The data for the Q[7]–**g**·HCl system can also fit to a 1:1 binding model (Fig. 5d and inset in Fig. 5d). By contrast, The addition of Q[8] to a solution of **g**·HCl at pH3.2 results in decreases in the peaks with a violet shift from 456 to 440 nm, with an isosbestic point at $\sim$535 nm (Fig. 5e). The differences of absorbance (ΔA) at the corresponding λ_{max}

vs. molar ratio of host Q[8] and guest $(N_{Q[8]}/N_{g·HCl})$ can be fitted to a 1:2 binding model (Fig. 5f). The data on absorbance change (ΔA) vs. ratio of $[N_{Q[8]}/(N_{Q[8]} + N_{g·HCl})]$ also confirm that the interaction between Q[8] with the selected guest can be fitted to a 1:2 binding model (inset in Fig. 5e). It should be noted that there is still a dip in the titration curve after the equivalence point. It could be caused by the equilibration of 1:2 complex and 1:1 complex of the host Q[8] and the guest **g**, in particular, with the increase of Q[8] after the equivalence point.

The measured data for the three inclusion host–guest systems enabled calculation of binding constants [25]. LogK values of 7.2 ± 0.1 for TMeQ[6]–**g**·HCl, 6.5 ± 0.1 for Q[7]–**g**·HCl and 10.7 ± 0.3 for Q[8]–**g**·HCl were obtained based on the absorption spectrophotometric analysis.

Crystal structures of the inclusion complexes of TMeQ[6]–g·HCl and Q[8]–g·HCl

Based on the studies on the interaction of the various Q[n] with the guest in solution, one can conclude that the hosts prefer to include the phenyl moiety rather than the m-phenylenediamine moiety of the selected guest. Crystal structures of the inclusion complexes can provide more details about the interaction between the Q[n] host and the **g**·HCl guest. In this work, two single crystal X-ray structures of the inclusion complexes TMeQ[6]–**g**·HCl and Q[8]–**g**·HCl were obtained. Both structures showed the phenyl moiety of the guest inserted into the host cavity, supporting the ^{1}H NMR spectroscopic study and spectrophotometric analysis in solution.

Figure 6 illustrates the structure of the TMeQ[6]–**g**·HCl adducts in the solid state. The phenyl moiety of the guest was clearly inserted into the cavity center of the host, whereas the m-phenylenediamine moiety lay in a portal zone of the host. Thus, the phenyl ring in the cavity underwent a shielding effect, and the corresponding proton resonances experienced a significant upfield shift (as observed in the ^{1}H NMR spectra discussed earlier). Moreover, the interaction between the portal hydrogen bonds of the protonated m-phenylenediamine moiety of the guest, with the rimmed carbonyls of TMeQ[6], increased the stability of the title inclusion complexes. Nevertheless it is unclear which N of the m-phenylenediamine moiety was protonated in solution.

Two inclusion complexes arranged in a pair and formed a dumbbell-like host–guest assembly exhibiting π–π stacking of two adjacent m-phenylenediamine moieties, hydrogen-bonding and ion–dipole interactions. In addition, the dumbbell-like host–guest assemblies were linked by hydrogen-bonding between portal carbonyl and latticed water molecules, to form a one-dimensional supramolecular chain as shown in Fig. 6. The distances between the amine nitrogens N27 and N28 of the guest and the portal

Fig. 5 Electronic absorption spectra of **g**·HCl
$(2 \times 10^{-5}$ mol/L) in the presence of Q[n] **a** TMeQ[6]: 1–14 $(0$–6.0×10^{-5} mol/L), **c** Q[7]: 1–16 $(0$–6.0×10^{-5} mol/L) and **e** Q[8]: 1–13 $(0$–4.4×10^{-5} mol/L) and corresponding ΔA–$N_{Q[n]}/N_g$ curves (Q[n](**b** TMeQ[6], **d** Q[7] and **f** Q[8]) (insert: ΔA–$N_{Q[n]}/(N_g + N_{Q[n]})$ curves) in aqueous solution (pH ≈ 3.2) at 456 nm
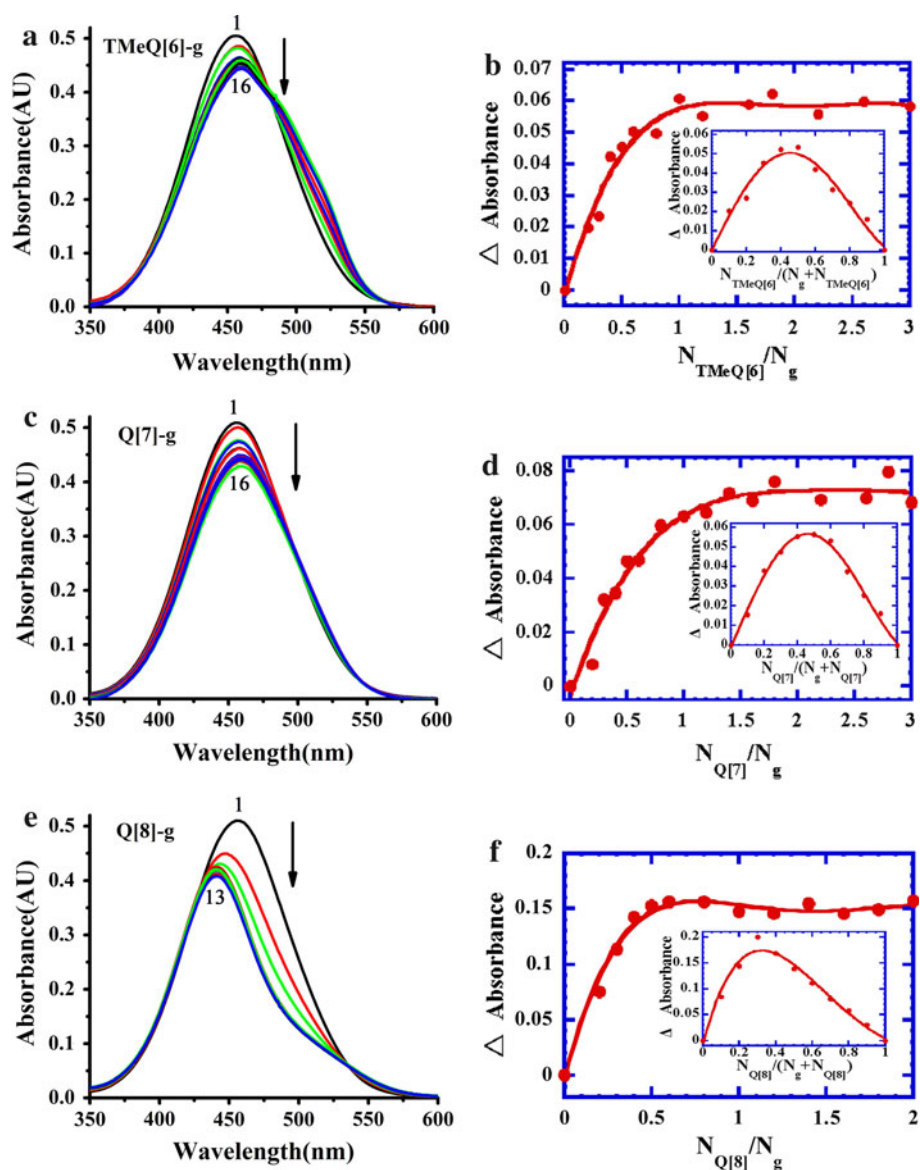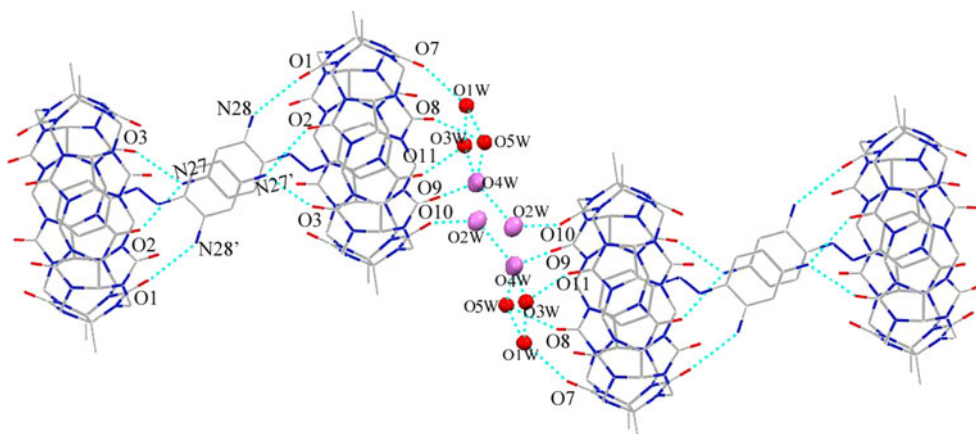

Fig. 6 Crystal structure of a 1D supramolecular chain constructed of dumbbells of TMeQ[6]–**g** inclusion complexes, through π–π stacking, hydrogen-bonding and ion–dipole interaction

carbonyl oxygen atoms of the host were 1.759 and 1.957 Å respectively, and the lengths of the related hydrogen bonds were 3.029 Å (N27···O2), 2.943 Å (N27···O3), and 2.887 Å (N28···O1), respectively. The distance between π···π stacked m-phenylenediamine moieties in the dumbbell-like host–guest assembly was 3.289 Å. The bond
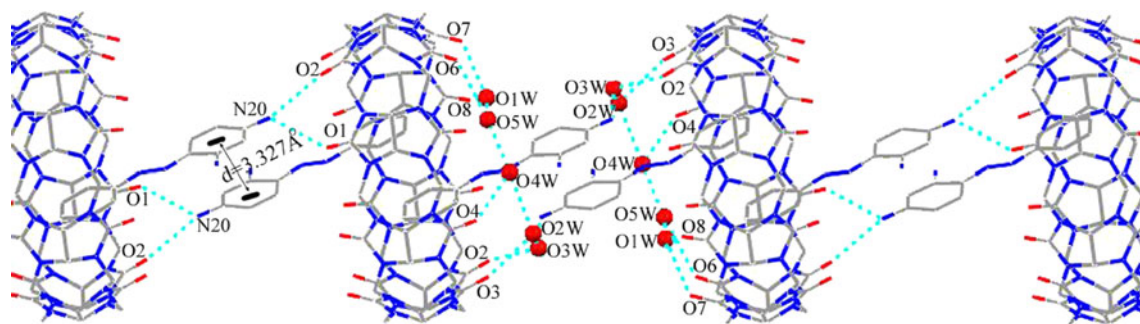
Fig. 7 Crystal structure of a 1D supramolecular chain constructed of Q[8]–**g** inclusion complexes

distances of the two pairs of hydrogen bonds connected the "dumbbell" were 2.735 Å (O9···O4W), 2.762 Å (O4 W···O2W), and 2.964 Å (Q2W···O10) respectively. Moreover, four water molecules (O1W, O4W, O7W and O11W) combined together to form a lid that covered the portal carbonyl oxygen atoms of the hosts, through hydrogen bonding between these carbonyl oxygen atoms and these water molecules.

When the Q[8]–**g**·HCl adduct was in the solid state, the phenyl moiety of a guest also intruded into the cavity center of the host, and each host Q[8] included two guests due to the larger cavity. The two m-phenylenediamine moieties of the two included guests in Q[8] protruded from two opening portals of Q[8] and the inclusion complex of Q[8]–**g**·HCl was symmetric. The two included phenyl moieties stacked in a parallel configuration, and the distance between the two aromatic rings was 3.840°. The inclusion complex with a 2:1 ratio of Q[8]:**g**·HCl was also linked through π-π stacking, hydrogen-bonding and ion–dipole interaction. This resulted in the formation of a supramolecular chain consisting of the inclusion complexes of Q[8]–**g**·HCl as shown in Fig. 7. The distance between the amine nitrogen N20 of the guest and the portal carbonyl plane of the host was 2.310 Å, and the bond distances of the related hydrogen bonds were 2.992 Å (N20···O1) and 2.977 Å (N20···O1) respectively. The spacing of π···π stacked m-phenylenediamine moieties in the dumbbell-like host–guest assembly was 3.365 Å. At the portals of host Q[8], a number of water molecules (O1W–O5W) formed a molecular complex through hydrogen bonding.

Conclusion

The interaction between TMeQ[6], Q[7], Q[8] and **g**·HCl in aqueous solution was investigated using ^{1}H NMR spectroscopy, electronic absorption spectroscopy, as well as single crystal X-ray diffraction. The ^{1}H NMR spectra analysis established a basic interaction, in which the host selectively bound the phenyl moiety of the guest. Absorption spectrophotometric analysis in aqueous solution defined the stability of the host–guest inclusion complexes quantitatively. At pH 3.2, logK values between 6 and 7 were obtained for the smaller hosts TMeQ[6] and Q[7], while a logK value of 10.7 was obtained with a host:guest ratio of 1:2 for host Q[8]. The single crystal X-ray structures of the inclusion complexes of TMeQ[6]–**g**·HCl and Q[8]–**g**·HCl showed that the phenyl moiety of the guest inserted into the host cavity. This finding supported the solution studies. The inclusion complex assembled as identified in the solution ^{1}H NMR studies and existed as stacked one-dimensional supramolecular chains.

References

1. Freeman, W.A., Mock, W.L.: Cucurbituril. J. Am. Chem. Soc. **103**, 7367–7368 (1981)
2. Day, A.I., Arnold, A.P., Blanch, R.J., Snushall, B.: Controlling factors in the synthesis of cucurbituril and its homologues. J. Org. Chem. **66**, 8094–8100 (2001)
3. Kim, J., Jung, I.S., Kim, S.Y., Lee, E., Kang, J.K., Sakamoto, S., Yamaguchi, K., Kim, K.: New cucurbituril homologues: syntheses, isolation, characterization, and X-ray crystal structures of cucurbit[n]uril (n = 5, 7, and 8). J. Am. Chem. Soc. **122**, 540–541 (2000)
4. Day, A.I., Blanch, R.J., Arnold, A.P., Lorenzo, S., Lewis, G.R., Dance, I.: A cucurbituril-based gyroscane: a new supramolecular form. Angew. Chem. Int. Ed. Engl. **41**, 275–277 (2002)
5. Zhao, Y.J., Xue, S.F., Zhu, Q.J., Tao, Z., Zhang, J.X., Wei, Z.B., Long, L.S., Hu, M.L., Xiao, H.P., Day, A.I.: Synthesis of a symmetrical tetrasubstituted cucurbit[6]uril and its host–guest compound with 2, 2′-bipyridine. Chin. Sci. Bull. **49**, 1111–1116 (2004)
6. Ma, P.H., Xiao, X., Zhang, Y.Q., Xue, S.F. Tao, Z.: 1,3,5, 7,9,11,13,15-Octaazapentacyclo [9.5.1.13,9.06,18.014,17]octadecane-4,8,12,16-tetrone monohydrate: a methylene-bridged glycoluril dimmer. Acta Cryst. E**64**, o1795 (2008)
7. Huang, W.H., Zavalij, P.Y., Isaacs, L.: Cucurbit[n]uril formation proceeds by step-growth cyclo-oligomerization. J. Am. Chem. Soc. **130**, 8446–8454 (2008)

8. Lagona, J., Mukhopadhyay, P., Chakrabarti, S., Isaacs, L.: The cucurbit[n]uril family. Angew. Chem. Int. Ed. **44**, 4844–4870 (2005)

9. Huang, F.H., Gibson, H.W.: Polypseudorotaxanes and polyrotaxanes. Prog. Polym. Sci. **30**, 982–1018 (2005)

10. Sokolov, M.N., Dybtsev, D.N., Fedin, V.P.: Supramolecular compounds of cucurbituril with molybdenum and tungsten chalcogenide cluster aqua complexes. Russ. Chem. Bell. **52**, 1041–1060 (2003)

11. Buschmann, H.J., Mutihac, L., Jansen, K.: Complexation of some amine compounds by macrocyclic receptors. J. Incl. Phenom. Macrocycl. Chem. **39**, 1–11 (2001)

12. Mock, W.L.: Cucurbituril. Top. Curr. Chem. **175**, 1–24 (1995)

13. Kim, K., Selvapalam, N., Oh, D.H.: Cucurbiturilsa new family of host molecules. J. Incl. Phenom. Macrocycl. Chem. **50**, 31–36 (2004)

14. Kim, K., Selvapalam, N., Ko, Y.H., Park, K.M., Kim, D., Kim, J.: Functionalized cucurbiturils and their applications. Chem. Soc. Rev. **36**, 267–279 (2007)

15. Pagga, U.: Testing biodegradability with standardized methods. Chemosphere **35**, 2953–2972 (1997)

16. Galliano, H., Gas, G., Sevis, J.L., Boudet, A.M.: Lignin degradation by *Rigidoporus lignosus* involves synergistic action of two oxidizing enzymes: Mn peroxidase and laccase. Enzyme Microb. Tech. **13**, 478–482 (1991)

17. Zimmermann, T., Kulla, H.G., Leisinger, T.: Properties of purified Orange II azoreductase, the enzyme initiating azo dye degradation by *Pseudomonas* KF46. Eur. J. Biochem. **129**, 197–203 (1982)

18. Shin, H.S., Ahn, H.S.: Determination of ethylene oxide–hemoglobin adduct by silylation and gas chromatography–electron impact-mass spectrometry. Chromatographia **843**, 202–208 (2006)

19. Buschmann, H.J., Schollmeyer, E.: Cucurbituril and β-cyclodextrin as hosts for the complexation of organic dyes. J. Incl. Phenom. Macrocycl. Chem. **29**, 167–174 (1997)

20. Liu, J.X., Tao, Z., Xue, S.F., Zhu, Q.J., Zhang, J.X.: Investigation of host-guest compounds of Cucurbit[$n = 5$–8]uril with some piperazine derivatives. Chin. J. Inorg. Chem. **20**, 139–146 (2003)

21. Zhao, Y.J., Xue, S.F., Zhu, Q.J., Tao, Z., Zhang, Y.Q., Zhang, J.X., Wei, Z.B., Long, L.-S.: Studies on the interaction of disubstituted Cucurbit[6]uril with 2-(aminomethyl)pyridine. Acta Chim. Sinica **63**, 913–918 (2005)

22. Ma, P.H., Tao, Z., Xue, S.F., Zhu, Q.J., Wang, S.K., Yuan, S.W., Zhang, J.X., Zhou, X.: Interaction of Cucurbit[n 6–8]urils with three *N*-benzyl Cage guests. Chin. J. Org. Chem. **27**, 414–418 (2007)

23. Feng, Y., Xiao, X., Xue, S.F., Zhang, Y.Q., Zhu, Q.J., Tao, Z., Lawrance, G.A., Wei, G.: Host-guest complex of a water soluble cucurbit[6]uril derivative with the hydrochloride salt of 3-amino-5-phenylpyrazole. Supramol. Chem. **20**, 517–525 (2008)

24. Huo, F.J., Yin, C.X., Yang, P.: The crystal structure, self-assembly, DNA-binding and cleavage studies of the [2]pseudorotaxane composed of cucurbit[6]uril. Bioorg. Med. Chem. Lett. **17**, 932–936 (2007)

25. Inoue, Y., Yanamoto, K., Wada, T., Everitt, S., Gao, X.M., Hou, Z.J., Tong, L.H., Jiang, S.K., Wu, H.M.: Inclusion complexation of (cyclo)alkanes and (cyclo)alkanols with 6-O-modified cyclodextrins. J. Chem. Soc. Perkin Trans. **2**, 1807–1816 (1998)